Variability of The Minimum Temperature Over Two Centuries In The Overlap Region Between The Fringe of The Asian Westerly Region and The Temperate Continental-Monsoon Climate Transition Zone

Bolin Sun (732625667@qq.com)
Inner Mongolia Agriculture University: Inner Mongolia Agricultural University https://orcid.org/0000-0002-5356-7620
Long Ma
Inner Mongolia Agricultural University https://orcid.org/0000-0002-4588-8918
Tingxi Liu
Inner Mongolia Agricultural University
Xing Huang
Inner Mongolia Agricultural University

Research Article

Keywords: mean minimum temperature; climate change, dendroclimatology, Asian westerly region, temperate continental-monsoon climate transition zone

Posted Date: December 1st, 2021

DOI: https://doi.org/10.21203/rs.3.rs-1089921/v1

Abstract

The overlap region between the eastern fringe of the Asian westerly region and the temperate continental-monsoon climate transition zone is sensitive to climate changes and is characterized by fragile ecosystems. It is necessary to uncover the patterns of long-term historical climate variability there. A standardized tree-ring width chronology was constructed based on the tree-ring samples collected from four representative tree species in four typical areas in the overlap region, and the 203- to 343-year annual mean minimum temperature series in the overlap region were reconstructed. The reconstructed series overlapped well with extreme climate events and low-temperature periods recorded in historical data. Therefore, the reconstructed model is stable and reliable. As suggested by the reconstructed series, the variability of annual mean minimum temperature was increasingly drastic from east to west in the overlap region, with gradually shorter periodicities. In the 19th century, the high-latitude area was in the high-temperature period, and the entire overlap region experienced significant low-temperature periods lasting 20–45 years till the 1950s. The western part had an earlier start time of low-temperature periods, longer cooling duration, and slower cooling rate than the central part. The overlap region experienced a significant warming period in approximately the last half-century, with temperature increasing faster in the western and eastern parts than in the central part. The temperature variability in the overlap region was more intense in the last two centuries, with shorter periodicities and a larger proportion of cold periods. The central and western parts of the Asian westerly region, the mid- to high-latitude regions of the transition zone, and the overlap region saw significantly low-temperature periods or drastic cooling trends (the Little Ice Age) in the first half of the 19th century and significant warming trends under global warming afterwards. The influences of these changes might have been exacerbated by the westerly circulation. This study not only provides new insight into the use of dendroclimatology to extract temperature series in the Asian westerly region and the transition zone but also serves as a reference for research on global climate change.

1 Introduction

Global climate change has a far-reaching impact on the living environment of humans and other living organisms (IPCC, 2014; Wada *et al.*, 2014). The instrumental recording of climatological data has a history of less than 100 years in most regions of the world. Therefore, proxy climate indicators are chosen for the analysis of historical climate variability. The Asian westerly region refers to the part of Asia dominated by the mid-latitude westerly circulation. The southeast fringe of the Asian westerly region is also part of the transition zone of the temperate continental-monsoon climate zone, which is one of the regions that responds the most sensitively to global climate change (Feng et al., 2014). At present, the characteristics and patterns of long-term historical climate variability in the overlap region between the fringe of the Asian westerly region and the temperate continental-monsoon climate transition zone (referred to as the overlap region hereinafter) remain unclear.

Since the establishment of dendrochronology by Andrew E. Douglass (Ph.D. in astronomy) at the University of Arizona in the 1920s, great progress has been made in the application of dendrochronology

to reconstructing climatological factors in various and periods based on the close relationship between tree ring growth and climatological signals (Liu et al., 2010; Kamenos et al., 2012). Such research has been done in many countries and regions on all continents except Antarctica using conifer species, such as *Pinus sylvestris* L. (Kirchhefer 2000; Gutiérrez 1989), *Pinus tabulaeformis* Carr. (Zhang et al., 2017b), *Picea schrenkiana* Fisch. (Zhang et al., 2017a). Past dendroclimatological studies produced fruitful scientific achievements. For example, scholars have discovered the close association between volcanic eruption and abrupt cooling events in the Northern Hemisphere in the past 600 years (Mann et al. 1998; Mann et al., 1999); the interactions between abrupt climate events, such as the Asian monsoon, Pacific Decadal Oscillation (PDO), and El Niño, over the last 400 years (D'Arrigo et al., 2005); and the significant exacerbation of droughts in North America under the influence of global warming (Cook et al., 2010).

In 1939, Rossby, a Swedish meteorologist, first proposed the concept of westerly circulation (Rossby *et al*., 1939), which forms when the warm air masses from the equator encounter the cold air masses from the poles. Central Asia is the region of the Northern Hemisphere most affected by westerly circulation. This region, known as the Asian westerly region, is located deep in the hinterland of the Eurasian continent, with a dry climate, limited rainfall, and extremely fragile ecosystems. There are many types of climate in the Eurasian continent, including temperate continental climate and temperate monsoon climate. A unique transition zone, called the temperate continental-monsoon climate transition zone (referred to as the transition zone hereinafter), forms at the border between the temperate continental climate and the temperate monsoon climate. This transition zone is extremely sensitive to climate changes under the joint influences of many geographical, hydrological, and climatological factors. Currently, the single-site dendroclimatological studies in the Asian westerly region and the transition zone mainly have used the tree-ring width data of conifer species such as *Larix gmelinii* (Rupr.) Kuzen. (Earle et al., 1994; Jiang et al., 2020), *Picea asperata* Mast. (Peng et al., 2020; Zhang et al., 2020) for the reconstruction of meteorological factors such as the mean temperature (Peng et al., 2020), mean minimum temperature (Jiang et al., 2020), and Palmer Drought Severity Index (PDSI) (Liu et al., 2017), in the central and northern parts of the Asian westerly region, including Southern Kazakhstan (Zhang et al., 2020), and Northwest China (Peng et al., 2020), and the middle- to high-latitude parts of the transition zone, including Northeast China (Jiang et al., 2020) and Siberia (Earle et al., 1994). The temperature variability over the last two centuries in the Asian westerly region and the transition zone were significantly affected by global climate change (Liu et al., 2017; Liang et al., 2018; Sun et al., 2019). The southeast fringe of the Asian westerly region and the low-latitude part of the transition zone overlaps in the western part of Inner Mongolia, China, forming a special climate in this overlap region. The temperature variability in this overlap region is extremely large due to the long-term joint influences of the fragile and variable climatic environment and complex and diverse geographical environments, which have greatly impacted the ecological environment and social development in this region. However, the long-term historical variability of climatological factors such as the mean minimum temperature, runoff, relative humidity, and precipitation in the eastern fringe of the Asian westerly region and the low-latitude parts of the transition zone, especially in the overlap region between the two, has been rarely investigated, and the characteristics and patterns of long-term historical climate variability in the overlap region awaits

further research. Therefore, multi-site studies in the overlap region are needed to reconstruct its long-term historical climate variability on a large spatial scale and to reveal the characteristics and patterns of climatological factors in this region over a long historical period.

To this end, four typical areas in the overlap region were selected as the sampling sites. Tree-ring samples were collected from four representative tree species for the construction of a tree-ring width chronology, and the 203- to 343-year temperature series in the overlap region were reconstructed to reveal the characteristics and patterns of temporal and spatial temperature variabilities in the overlap region. The results were compared with the results of existing studies on the Asian westerly region and the transition zone. Our findings not only provide new insight into the use of dendroclimatology to extract temperature series in the Asian westerly region and the transition zone but also serve as a reference for research on global climate change.

2 Data And Methods

2.1 Overview of the study area

The sampling area is in the overlap region between the southeast fringe of the Asian westerly region and the low-latitude part of the transition zone (Figure 1). Specifically, it is the middle and west part of Inner Mongolia, and it has a large east–west span. This area has annual precipitation of 50 mm in its westernmost part and approximately 400 mm in the easternmost part. There are significant temperature variations throughout the area (Figure 2). The climate types in this area are complex and diverse because of the joint influences of the westerly circulation in the Northern Hemisphere and the temperate continental climate and temperate monsoon climate. It is a typical cold and semi-arid to arid area, with a sensitive and fragile climatic environment. In this study, tree-ring samples for dendroclimatological study were collected from four sites in the overlap region: the lower reaches of the Heihe River, Helan Mountains, Yinshan Mountains, and the northern piedmont of the Daxinganling Mountains.

2.2 Reconstruction of the chronology using proxy materials and tree-ring data

Tree-ring samples were collected from dominant tree species *Populus euphratica* Oliv., *P. asperata* Mast., *Platycladus orientalis* (L.) Franco, and *Ulmus pumila* L., from west to east, in the Bayantaolaisumu region in the downstream region of the Heihe River, the Nansi region west to the Helan Mountains, the Dahuabei region of Wulashan Mountain in the Yinshan Mountains, and the Wolongquan region in the northern piedmont of the Daxinganling Mountains in July 2017. Sampling was performed in strict accordance with the sampling standards of the International Tree-Ring Database (ITRDB). A total of 342 samples were collected from 169 trees during the sampling process (at least two samples from each tree) (Figure 3b). After the collected samples were naturally dried indoors, they were polished using a set of dry sandpapers from coarse to fine until the sample surfaces were smooth and the tree rings were clearly visible. Polished samples were scanned using a high-resolution (10,200×14,039) scanner. The obtained

data were analysed using WinDENDRO software (accuracy of 0.001 mm) for cross-dating, and the calendar year for each ring was accurately determined. The quality of cross-dating was controlled using the internationally accepted COFECHA procedure (Holmes et al., 1983), which involves examining missed rings, false rings, and dating errors. The ARSTAN (Cook 1985) program was used to remove the interference from tree growth trends and non-climatic variables. To retain as many low-frequency signals as possible, detrending was performed mainly using the negative exponential curve method, with spline functions used for some samples. Last, a conventional standardized chronology (Figure 3) was synthesized using double-weighted means of the detrended series. The subsample signal strength (SSS) was used to determine the minimum number of replicas for a reliable chronology (Fritts 1976). The reliable portion of the chronology was defined in this study as the part of the chronology where SSS was > 0.85 to ensure the maximum length of the reconstructed series and its reliability. The quality of the standardized chronology was evaluated by statistical indicators such as the mean correlation between trees, mean sensitivity, and signal-to-noise ratio of the chronology.

2.3 Climatological data collection

The monthly and annual mean temperature, minimum temperature, maximum temperature, and precipitation in the datasets of the Abaqi Banner, Baotou, Ejina, and Jilantai climatological stations close to the four sampling sites were obtained from the National Meteorological Information Centre (http://data.cma.cn/).

2.4 Data analysis method

(1) Corresponding data from adjacent stations were used for missing data, and correlation analysis and regression analysis were used for interpolation and expansion.

(2) The Pearson correlation coefficient was calculated to analyse the correlations between the tree-ring index and climatological factors.

(3) The long-term historical temperature series was reconstructed using linear regression.

(4) The integrity and reliability of the reconstructed model were tested using the split-sample method, which is widely used in dendrochronological studies (Fritts, 1976; Cook et al., 1999). The statistical parameters used in this study included Pearson's correlation coefficient (r), R-squared (R^2), the sign test (ST) value, reduction of error (RE), coefficient of efficiency (CE), and the product means test (t) value. RE and CE can be used to accurately test the reliability of reconstructed values. Positive RE and CE values indicate that the reconstructed model has a certain predictive ability, and the closer the two values are to 1, the stronger is the predictive ability of the reconstructed model. ST can be used to test the similarity between the between the low-frequency signals of the reconstructed values and those of the measured values by calculating the number of times when the anomalies of the reconstructed and measured values have the same or opposite sign. t evaluates the signs and magnitudes of the anomalies of the reconstructed and measured values and thus can intuitively reflect the hydroclimatological information in the reconstructed values.

(5) The Z-score method was used for the standardization of the reconstructed historical temperature series using the following calculation formula:

$$\text{Z-score} = (\mathrm{R} - \mathrm{MN}) / \mathrm{SD}$$

In the formula, R is the reconstructed temperature, °C;MN is the mean of the temperature series, °C; and SD is the standard deviation of the reconstructed temperature series, °C.

(6) The covariance coefficient of variation (CV) was used to represent the strength of variability of the reconstructed historical temperature series. CV was calculated by the following formula:

$$\mathrm{CV} = |\mathrm{SD} / \mathrm{MN}|$$

where SD is the standard deviation of the reconstructed historical temperature series, °C; and MN is the mean value of the reconstructed historical temperature series, °C.

(7) The tendency rate was used for the analysis of temperature trends.

(8) The periodic variability of the reconstructed historical temperature series was analysed using the Morlet wavelet (Venugopal *et al.*, 1996), which is defined as follows:

$$\psi(t) = Ce^{-t^2/2}\cos 5t$$

The scale factor (a) of Morlet wavelet and periodicity (T) have the following relationship:

$$\mathrm{T} = \left[\frac{4\pi}{\omega_0 \sqrt{2 + \omega_0^2}} \right] \times a$$

where ω_0 is usually an empirical value close to 6.2.

(9) The Mann-Kendall nonparametric statistical method was used to detect any abrupt changes in the reconstructed temperature series (Fu *et al.*, 1992).

(10) The annual temperature series and the segmented trendline or the series in 3- to 5-year sliding windows and the segmented trendline were used to identify the years of a warming hiatus after an abrupt temperature change. If the tendency rate of a certain year after the abrupt change reaches the maximum and reaches 0.1°C/10a at the end of the series (2016), then this year is a warming hiatus. If the tendency rate after the abrupt change is negative, then this year is a cooling hiatus.

The data in (1)–(7) and (10) were analysed using Excel and SPSS, and the data in (8)–(9) were analysed using via MATLAB scripts.

3 Results And Discussion

3.1 Relationship between tree-ring growth and hydroclimatological factors in each sampling site

The correlation coefficients between the tree-ring indices of different tree species and hydroclimatological factors are shown in Figure 4.

Figure 4 shows that the tree-ring index of each region is closely associated with the local temperature. The tree-ring indices had a negative correlation with the annual and monthly means of the three air-temperature measures (mean temperature, mean maximum temperature, and mean minimum temperature) in all region/time pairs except the Wolongquan region and the Ejina region in March, April, and June. Temperature in the arid and semiarid areas in the middle and west parts of the study area can affect tree-ring growth by affecting factors such as soil water conditions and the respiration and transpiration rates of trees (Li et al, 2000; Yu et al, 2011).

Overall, the radial growth of the trees in each sampling site showed a significant positive/negative correlation with the three temperature measures (Figure 4). The coefficients of correlation between radial growth and the annual means of the three temperature measures were higher than those between radial growth and the monthly means of the three temperature measures. The radial growth in all sampling sites exhibited a significant correlation with annual mean minimum temperature (correlation coefficients: -0.448, -0.41, -0.87, and 0.801). The coefficients of correlation between radial growth and the annual means of the three temperature measures followed the descending order of annual mean minimum temperature > annual mean temperature> annual mean maximum temperature. The radial growth generally had low coefficients of correlation with the annual and monthly precipitation series, far below the coefficients of correlation between radial growth and temperature, and it had alternating positive/negative correlations. The coefficients of correlation between radial growth and the monthly means of the three temperature measures followed the descending order of monthly mean minimum temperature > monthly mean temperature > monthly mean maximum temperature. The radial growth of *P. euphratica* Oliv. in the Ejina region had higher responses to the three temperature measures in January and February (mean correlation coefficient: -0.435, -0.383) than in other months, and the three temperature measures in March–September generally had a weak limiting effect on the radial growth of *P. euphratica* Oliv. The responses of the radial growth of *P. asperata* Mast. in the Helan Mountains to monthly mean minimum temperature response were strongest in June (0.353) and October (-0.408), and the responses of the radial growth of *P. asperata* Mast. to the three temperature measures were weakest in March and April. The radial growth of *P. orientalis* (L.) Franco in Wulashan Mountain generally had strong responses to the three temperature measures (all reached 95% significance), indicating that the three temperature measures had a strong limiting effect on the radial growth of *P. orientalis* (L.) Franco. In contrast, the radial growth of *Ulmus pumila* L. in the Wolongquan region generally had a positive correlation with the three temperature measures (except the mean maximum temperatures in October and

November), and the contributions of the three temperature measures to the radial growth of *Ulmus pumila* L. were higher in May to August than in other months.

In summary, the correlation between different tree species and the annual means of the three temperature measures in different regions was stronger than the correlation between different tree species and the monthly means of the three temperature measures. The limiting effects of the three temperature measures on radial growth were stronger in the eastern region than in the western region, following the descending order of mean minimum temperature > mean temperature > mean maximum temperature. The three types generally had negative correlations with the radial growth of trees of temperatures in all sampling sites except the Wolongquan region in the easternmost part of the study area. We attribute this phenomenon to the following two causes. First, the accumulated snow in winter is an important driving force for tree growth in areas with limited precipitation during the growing season (Adrià et al., 2015; Yu et al., 2013), and the snowmelt volume and time have an important ecological impact by influencing tree growth (Adrià et al., 2015). An increase in minimum temperature in the study area may lead to an increase in snowmelt in winter and thus reduce the snowmelt volume in the growing season, making the water supply insufficient in the growing season. In the summer, when the temperature peaks, the water content in the soil becomes more difficult to preserve, ultimately leading to narrow tree-rings (Yu et al., 2013). Second, this phenomenon has been observed in cold and arid plateau areas, such as the Sichuan–Tibet plateau region (Thapa et al., 2014), eastern Inner Mongolia (Ma et al., 2015a), and the Qilian Mountains (Ma et al., 2015b) of China, indicating that the radial growth of trees in cold and arid plateau areas may respond negatively to temperature. As a typical arid and semiarid area, the study area has low precipitation during the early stage of tree growth (April to May), and evaporation becomes more intense as the temperature rises, which directly leads to the loss of soil water and greatly limits the growth of trees. June to August is the peak period of tree growth in the study area. The favourable heat and water conditions in this period rapidly promote the growth of trees. However, the temperature in this period is highest, resulting in the highest evaporation in the whole year, making soil water more difficult to preserve. As shown in Figure 4, the radial growth of the trees in this period responded strongly to temperature but weakly to precipitation.

3.2 Reconstruction of the annual mean minimum temperature

The correlation analysis showed that the correlation between the tree-ring index of each region and the annual mean minimum temperature in the corresponding region was strong. The annual mean minimum temperature series in each region was reconstructed using a linear regression equation. The reconstruction equations and relevant parameters are shown in Table 2. In the equation, T_i is the annual mean minimum temperature in the i^{th} year, °C; and I_t is the tree-ring index in the t^{th} year.

Table 1
Standardized chronology and statistical indicators in each sampling site

Statistical indicators	Statistic			
	HHR	HHM	WLM	WLL
Average value	1.000	1.000	1.000	1.000
Median	0.832	0.745	0.941	0.843
Skewness	0.939	0.363	0.987	0.746
Kurtosis	1.974	1.159	1.974	1.832
Mean sensitivity	0.363	0.426	0.193	0.326
Standard deviation	0.332	0.153	0.312	0.388
The first-order autocorrelation coefficient	0.504	0.651	0.604	0.560
The average correlation coefficient between each sequence and the main sequence	0.561	0.657	0.661	0.671
Mean correlation coefficient between trees	0.438	0.434	0.359	0.539
SNR(Signal to Noise Ratio)	13.122	16.158	15.122	14.133
Overall representativeness of samples	0.724	0.946	0.925	0.691
The first principal component explains the variance %	41.672	20.351	40.384	53.424
First year of subsample with signal strength >0.85	1796	1788	1666	1813

Table 2
Annual mean minimum temperature reconstruction equations and relevant parameters for different regions

Serial number	The reconstruction equation	*r*	N	R^2_{adj}	*F*	Significance level
HHR	$T_i = 1.949I_t + 3.120$	0.448	66	0.476	21.35	$p<0.001$
HLM	$T_i = -0.592I_t + 3.966$	0.41		0.464	31.88	
WLM	$T_i = -2.525I_t + 3.175$	0.87		0.754	49.803	
WLL	$T_i = 18.869I_t + 23.481$	0.801		0.552	18.84	

From the above parameters for reconstruction and the comparative analysis of reconstructed and measured values in different regions in Figure 5, the temporal and spatial variabilities of the reconstructed and measured series are consistent. The reconstructed series was divided into two periods, i.e., 1951–1983 and 1984–2016, which served as the calibration period and testing period. During the testing period, the RE and CE of the reconstructed results were positive in each period, and the RE was close to 1, indicating that the regression model had high predictive ability (Fritts 1991; Fritts 1976). Both

ST and the first-order difference sign test (ST_1) were significant at the 95% confidence level, indicating that the reconstructed series and the measured series were consistent in high- and low-frequency variabilities. During the calibration period, the r and t between the measured series and the reconstructed series reached 95% significance in each period, indicating that the reconstructed values contain more information on hydrological factors. In summary, the reconstruction equations for the four regions are stable and reliable and can accurately reconstruct the historical series of mean annual minimum temperatures in the study region.

3.3 Analysis of the spatial and temporal variability of the annual mean minimum temperature

The reconstructed series of the annual mean minimum temperatures in different regions in 1800–2016 were compared and analysed. In general, the mean minimum temperature in each region showed multiple cooling and warming cycles in the last 200 years (Figure 6). As shown by the trends in an 11-year sliding window, the mean minimum temperature in each region generally experienced an increasing–decreasing–increasing trend, i.e., the annual mean temperature variability in the study area had a certain synchronicity, with differences in the occurrence time of cooling and warming periods.

From the perspective of the trends in different time periods, the annual mean minimum temperature showed a rapid upward trend in all regions except the Helan Mountains in the 1920s and exhibited a continuously decreasing trend afterwards. The mean minimum temperature began to rapidly rise after the first abrupt change in the Helan Mountains of the last 200 years occurred, in 1821, and it started to decrease continuously in 1846, with the duration of cooling significantly longer in the west part than in the east part. The reconstructed series of all regions revealed abrupt changes from the end of the 19th century to the early 20th century. The temperature in the Wulashan and Wolongquan areas changed from a continuous decreasing trend to an increasing trend, and the increasing trend lasted for 30 years and 61 years in these two areas, respectively. Afterwards, the temperature decreased again. After the approximately 100-year cooling trends in the Ejina region and Helan Mountains ended by the middle of the 20th century, the Ejina region entered a rapid warming trend, while the Helan Mountains entered a slow warming trend, and the Wulashan Mountain and Wolongquan region also entered warming trends. In the early 1980s, the warming trend became gentler and turned into a weak cooling trend in all regions except the Wolongquan region where the warming trend continued, which is closely related to the warming hiatus in the Wolongquan area at the end of the 20th century (Liang et al., 2018; Sun et al., 2019).

In summary, from the end of the 19th century to the middle of the 20th century, each region experienced significant low-temperature periods of 20–45 years, which occurred increasingly earlier from west to east. The increasing/decreasing trends of the annual mean minimum temperature were increasingly longer from east to west (Figure 6), and the increasing trends were more significant but occurred 20–30 years later than the decreasing trends. The variability of the reconstructed series became increasingly intense from east to west, with periodicities gradually decreasing from 35–50 years to below 20 years. The

variations in the annual mean minimum temperature were longer and stronger in the west part of the study area than in the east part, perhaps because the western part of the study area was closer to the core area of the Asian Westerly Region (Feng et al., 2014). The study area experienced a significant warming trend in the last 100 years due to global warming, while the warming trends were most significant in the Ejina region in the west part of the study area and Wolongquan region in the east part and more gentle in the central area.

3.4 Comparison between the reconstructed results and historical climate events in other regions of the Asian Westerly Region and the transition zone

As shown by the comparison between our reconstructed results and the meteorological events recorded in the historical data in local and surrounding areas, most of the reconstructed minimum temperature series for the four representative areas in the overlap region well matched the frost disasters and dry periods recorded in the historical data (The Compilation of China Meteorological Disaster Canon, 2006; Li *et al*., 1998; Li *et al*., 2010; Wen *et al*., 2008). For example, the severe frost disaster in July 1897 widely damaged the crops in the Helan Mountains (-0.814°C) and Leping and Baode Prefectures (currently Xinzhou city, Shanxi Province). The cold wave and frost events in central and western Inner Mongolia in 1935–1951 basically overlapped with the last cooling period in the reconstructed series of the Wulashan area (1937–1951). A significant dry period in Baotou during 1747–1750 corresponds to the drastic warming period in the reconstructed series of the Wulashan region. During 1908–1909 and 1926–1928, most of Inner Mongolia experienced strong winds in spring and summer and persistent drought in spring, which led to poor harvests and abandoned farmland due to the lack of crop seeds, and the two periods are basically consistent with the second warming period (1908–1926) in the reconstructed series of the Wulashan region. In 1912, China entered the Republican Era, and the government called on the people to develop the Great Northwest of China, promoting activities such as water conservancy construction and afforestation in the downstream regions of the Heihe River. These human interventions helped protect the ecological environment of the basin, and the increased vegetation cover led to a continuous decrease in temperature.

In summary, these results indicate that the low-temperature periods and the dry periods recorded in the historical data are all reflected in the reconstructed series, indicating that the reconstructed annual mean minimum temperature series are reliable and can accurately represent the regional temperature variability.

The reconstructed temperature series in this study were compared with the existing reconstructed temperature series for the central and western parts of the Asian westerly region and the mid- and high-latitude regions in the transition zone to comprehensively and intuitively demonstrate the temporal and spatial variability in temperature in the overlap region (Figure 7). Figure 8a shows the reconstructed June-August annual mean temperature series from 1850 to 2015 for Southern Kazakhstan (HST, a high-latitude region in the transition zone) (Zhang et al., 2020). Figure 8b is the reconstructed annual mean

temperature series from 1766 to 2017 for Tianshan mountain, Xinjiang (TSM, a region in the central core area of the Asian westerly region) (Peng et al., 2020). Figure 8c shows the annual mean minimum temperature series from 1765 to 2013 for Hulunbuir area in northeast China (CET, middle-latitude parts of the transition zone) (Jiang et al., 2020). Figure 8d shows the summer mean temperature series in the Koryma River Basin from 1550 to 1989 for the Eastern Siberia (EST, high-latitude parts of the transition zone) (Earle et al., 1994).

Overall, the variabilities of reconstructed series were more intense in the overlap region, the high-latitude part of the transition zone, and the central part of the Asian westerly region (CV_{EST} = 23.3%, CV_{TSM} = 22.7%, $CV_{Mean\ (STA)}$ = 36.1%) than in the mid-latitude part of the transition zone and the western part of the Asian westerly region (CV_{CET} = 16.5%, CV_{HST} = 13.1%). As shown by the comparison between these reconstructed series in the shared period of nearly 200 years, the proportions of the cooling periods were 18–27% in the overlap region and 18–20% in the central and western parts of the Asian westerly region. The proportions of cooling periods were basically the same as those of the warming periods in the mid- and high-latitude parts of the transition zone. The periodicities in the overlap region were mostly below 60 years, which were shorter than the periodicities in other regions. Considering different periods, temperatures in all regions were relatively lower or showed a cooling trend from the mid-18th century to the mid-19th century, and the low-temperature periods lasted longer in the overlap region, the central part of the Asian westerly region, and the high-latitude part of the transition zone. This period is commonly called the Little Ice Age (Tkachuck, 1983). Since the second industrial revolution in the second half of the 19th century, the annual mean minimum temperature changed from rapid warming to slow cooling in the overlap region (except WLS), while it continued to warm in areas outside the overlap region, with the warming tends increasingly longer from low latitudes to high latitudes (Figure 8). In the first half of the 20th century, all regions experienced significant cooling trends, which are characterized by longer duration in the low- and high-altitude parts of the transition zone and a faster cooling rate in the middle the Asian westerly region and overlap region, as well as global warming. In the late of the 20th century, almost all series reached their peak values successively (except CET), and the warming trends were most significant and longest in the Asian westerly region and the central and western parts of the overlap region. In the early 21st century, a warming hiatus occurred throughout the overlap region except in its eastern part.

4 Conclusions

(1) The 203-to-343-year annual mean minimum temperature series in the overlap region were reconstructed based on the tree-ring width chronology of four tree representative species in four typical areas in the overlap region. The reconstruction equation and the reconstructed results are stable and reliable. The findings of this study bring new insight to the use of dendroclimatology in climatological research in these two special climate regions and fill the gap in the reconstruction of the long-term historical mean minimum temperature series in the overlap region over the last four centuries.

(2) In the last 200 years, the variability of the annual mean minimum temperatures in the overlap region was becoming more intense from east to west, with gradually shorter periodicities. In the 19th century, the high-latitude regions in the overlap region were in the high-temperature period, and all experienced the transition from warming trends to cooling trends. The entire overlap region experienced significant low-temperature periods of 20–45 years till the 1950s, with the occurrence of the low-temperature periods increasingly earlier from west to central, the cooling trend gradually shorter, and the cooling rate increasingly faster. The overlap region experienced a significant warming period in the last >50 years of the last century, and the warming rates in the western and eastern parts were faster than that in the central part.

(3) The reconstructed series overlap well with the extreme climate events and low-temperature periods recorded in local historical data and thus are reliable and can be used to represent regional temperature variability. As shown by at the variabilities of annual mean minimum temperatures over the past two centuries, the temperature variability was more intense in the overlap region, with higher proportions of cooling periods and shorter periodicities. In the first half of the 19th century, the central and western parts of the Asian westerly region, the mid- and high-latitude parts of the transition zone, and the overlap region all experienced significant low-temperature periods or cooling trends (Little Ice Age) and then entered significant warming trends under global warming. In addition, the warming trends lasted longer in different parts of the Asian westerly region, and some parts had higher warming rates, indicating that westerly circulation may exacerbate the impact of global warming.

Declarations

Competing interests

The authors declare that they have no conflict of interest.

Acknowledgements

This research was supported by the Natural Science Foundation of China (Grant No. 52069019 and 51669016). We are grateful for their support.

Code and data availability

The raw and processed data required to reproduce these findings cannot be shared at this time as the data also forms part of an ongoing study.

References

1. Adrià B, Monica M, Romà C, Jordi O, Josep VEDT (2015) The combined effects of a long-termexperimental drought and an extreme drought on the use of plant-water sources in a Mediterranean forest. Global Change Biology 21:1213–1122

2. Akkemik Ü, D'Arrigo R, Cherubini P, Köse N, Jacoby GC (2008) Tree-ring reconstructions of precipitation and streamflow for north-western Turkey. International Journal of Climatology: A Journal of the Royal Meteorological Society 28(2):173–183
3. Cook ER, Jacoby GC (1983) Potomac River streamflow since 1730 as reconstructed by tree rings. J Climate Appl Meteorol 22(10):1659–1672
4. Cook ER, Anchukaitis KJ, Buckley BM, D'Arrigo RD, Jacoby GC, Wright WE (2010) Asian monsoon failure and megadrought during the last millennium. Science 328(5977):486–489
5. Cook ER (1985) A time series analysis approach to tree-ring standardization. University of Arizona Press, Tucson
6. D'Arrigo R, Wilson R, Deser C, Wiles G, Cook E, Villalba R, Linsley B (2005) Tropical–North Pacific climate linkages over the past four centuries. J Clim 18:5253–5265
7. Earle CJ, Brubaker LB, Lozhkin AV, Anderson PM (1994) Summer temperature since 1600 for the upper Kolyma region, northeastern Russia, reconstructed from tree rings. Arct Alp Res 26(1):60–65
8. Feng S, Hu Q, Huang W, Ho CH, Li R, Tang Z (2014) Projected climate regime shift under future global warming from multi-model, multi-scenario CMIP5 simulations. Glob Planet Change 112:41–52
9. Fritts HC (1976) Tree rings and climate. Academic Press Inc, (London) Ltd., London, UK
10. Fritts HC (1991) Rconstuction large-scale climate patterns from tree-ring data. The University of Arizona Press, Tucson
11. Fu C (1992) The definition and detection of the abrupt climatic change. Sci Atmos Sin 16:482–493
12. Gutiérrez ME, Robertson CS (2011) Dendroclimatology of yellow cedar (Callitropsis nootkatensis) in the Pacific Northwest of North America, 1989
13. Holmes RL (1983) Computer-assisted quality control in tree-ring dating and measurement. Tree-ring Bulletin 43:69–78
14. IPCC (2014) Climate Change. "Mitigation of climate change.": Contribution of working group III to the fifth assessment report of the intergovernmental panel on climate change,
15. Jiang Y, Liu C, Zhang J, Han S, Coombs CE, Wang X, Wang J, Hao L, Dong S (2020) Tree ring width-based January–March mean minimum temperature reconstruction from Larix gmelinii in the Greater Khingan Mountains, China since AD 1765.*International Journal of Climatology*.
16. Kamenos NA, Hoey TB, Nienow P, Fallick AE, Claverie T (2012) Reconstructing Greenland ice sheet runoff using coralline algae. Geology 40(12):1095–1098
17. Kirchhefer AJ (2000) : Dendroclimatology on Scots pine (Pinus sylvestris L.) in northern Norway,
18. Li J (2010) Study on the historical evolution of ecological environment in Heihe River Basin. Doctoral dissertation, Zhejiang Normal University
19. Li J, Yuan Y, You X (2000) Research and application of dendrohydrology. Science Press, Beijing
20. Li S (1998) Records of Ejin Banner. Local records Publishing House
21. Liang LT, Ma L, Liu TX, Sun BL, Zhou Y (2018) Spatiotemporal variation of the temperature mutation and warming hiatus over northern China during 1951~2014 (in Chinese). China Environmental

Science 38:1601–1615

22. Liu Y, Sun J, Song H, Cai Q, Bao G, Li X (2010) Tree-ring hydrologic reconstructions for the Heihe River watershed, western China since AD 1430. Water Res 44(9):2781–2792
23. Liu Y, Zhang X, Song H, Cai Q, Li Q, Zhao B, Mei R (2017) Tree-ring-width-based PDSI reconstruction for central Inner Mongolia, China over the past 333 years. Clim Dyn 48:867–879
24. Ma L, Liu T, Wang J, Ji L, Gao R (2015a) Determining changes in the average minimum winter temperature of Horqin Sandy Land using tree ring records. Theor Appl Climatol 123:703–710
25. Ma Y, Liu Y, Song H, Sun J, Lei Y, Wang Y (2015b) A Standardized Precipitation Evapotranspiration Index Reconstruction in the Taihe Mountains Using Tree-Ring Widths for the Last 283 Years. PLoS One 10:e0133605
26. Mann ME, Bradley RS, Hughes MK (1998) Global-scale temperature patterns and climate forcing over the past six centuries. Nature 392:779–787
27. Mann ME, Bradley RS, Hughes MK (1999) Northern hemisphere temperatures during the past millennium: Inferences, uncertainties, and limitations. Geophys Res Lett 26:759–762
28. Peng Z, Qin L, Li X, Zhang H, Chen Y, Liu R, Zhang R (2020) Tree-ring-based temperature reconstruction since 1766 CE in the eastern Tianshan Mountains, arid Central Asia. Theoret Appl Climatol 142(1):687–699
29. Rossby CG (1939) Relation between variations in the intensity of the zonal circulation of the atmosphere and the displacements of the semi-permanent centers of action. J Mar Res 2:38–55
30. Sun BL, Feng MAL, Qi, Liu TX, Liang LT, Li HY, Zhou Y, Liu Y (2019) : Response of the warming hiatus to changing influences over the Inner Mongolia Autonomous Region. China Environmental Science. 39(05), 2131-2142, 2019
31. Thapa UK, Shah SK, Gaire NP, Bhuju DR (2014) Spring temperatures in the far-western Nepal Himalaya since AD 1640 reconstructed from Picea smithiana tree-ring widths. Clim Dyn 45:1–13
32. The compilation of China meteorological disaster Canon (2006) China meteorological disaster Canon. China Meteorological Press, Beijing. (in Chinese).
33. Tkachuck RD (1983) The little Ice Age. Origins 10(2):51–65
34. Venugopal V, Foufoula-Georgiou E (1996) Energy decomposition of rainfall in the time-frequency-scale domain using wavelet packets. J Hydrol 187(1–2):3–27
35. Wada Y, Bierkens MF (2014) Sustainability of global water use: past reconstruction and future projections. Environmental Research Letters 9(10):104003
36. Wen K (2008) The compilation of China meteorological disaster Canon. China Meteorological Press, Beijing. (in Chinese).
37. Yu D, Wang Q, Wang Y, Zhou W, Ding H, Fang X, Jiang S, Dai L (2011) Climatic effects on radial growth of major tree species on Changbai Mountain. Ann Forest Sci 68:921–933
38. Yu Z, Liu S, Wang J, Sun P, Liu W, Hartley DS (2013) Effects of seasonal snow on the growing season of temperate vegetation in China. Global Change Biology 19:2182–2219

39. Zhang R, Yuan Y, Yu S, Chen F, Zhang T (2017a) Past changes of spring drought in the inner Tianshan Mountains, China, as recorded by tree rings. Boreas 46(4):688–696
40. Zhang R, Qin L, Shang H, Yu S, Gou X, Mambetov BT, Bolatov K, Zheng WJ, Ainur U, Bolatova A (2020) Climatic change in southern Kazakhstan since 1850 CE inferred from tree rings.*International Journal of Biometeorology*,1–11
41. Zhang X, Liu Y, Song H, Cai Q, Li Q, Zhao B, Mei R (2017b) Interannual variability of PDSI from tree-ring widths for the past 278 years in Baotou, China. Trees 31:1531–1541

Figures

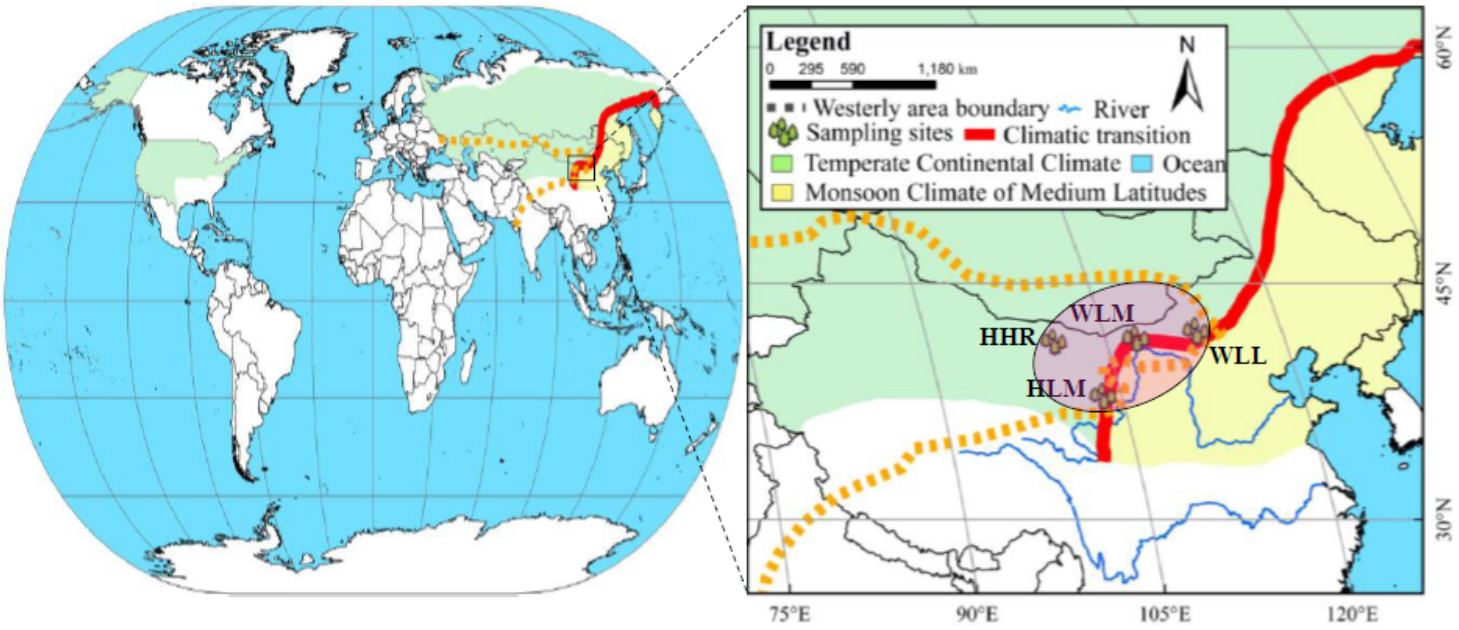

Figure 1

Distribution of climate types and sampling sites in the study area

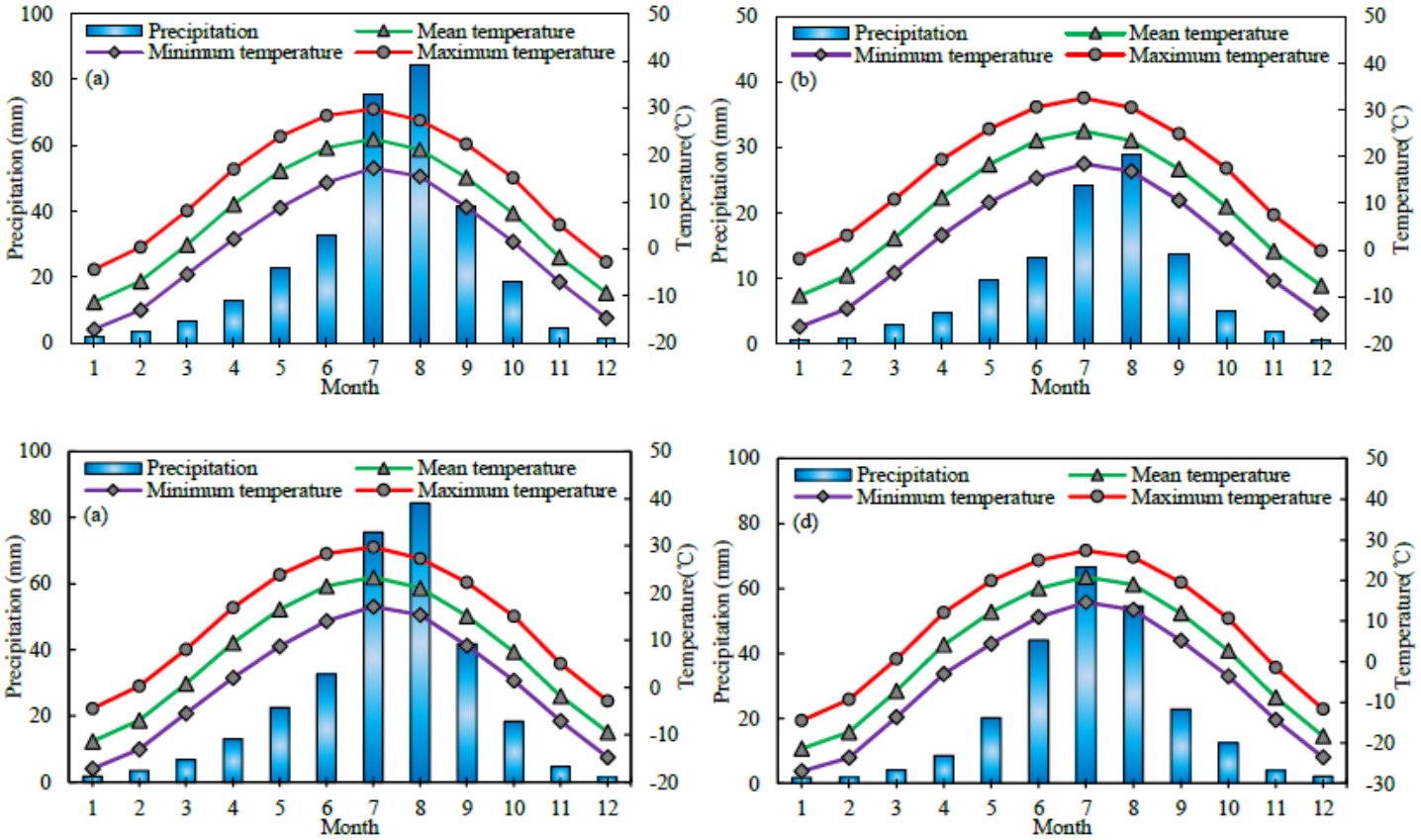

Figure 2

Distribution of mean monthly hydroclimatological data in each sampling area of the study area

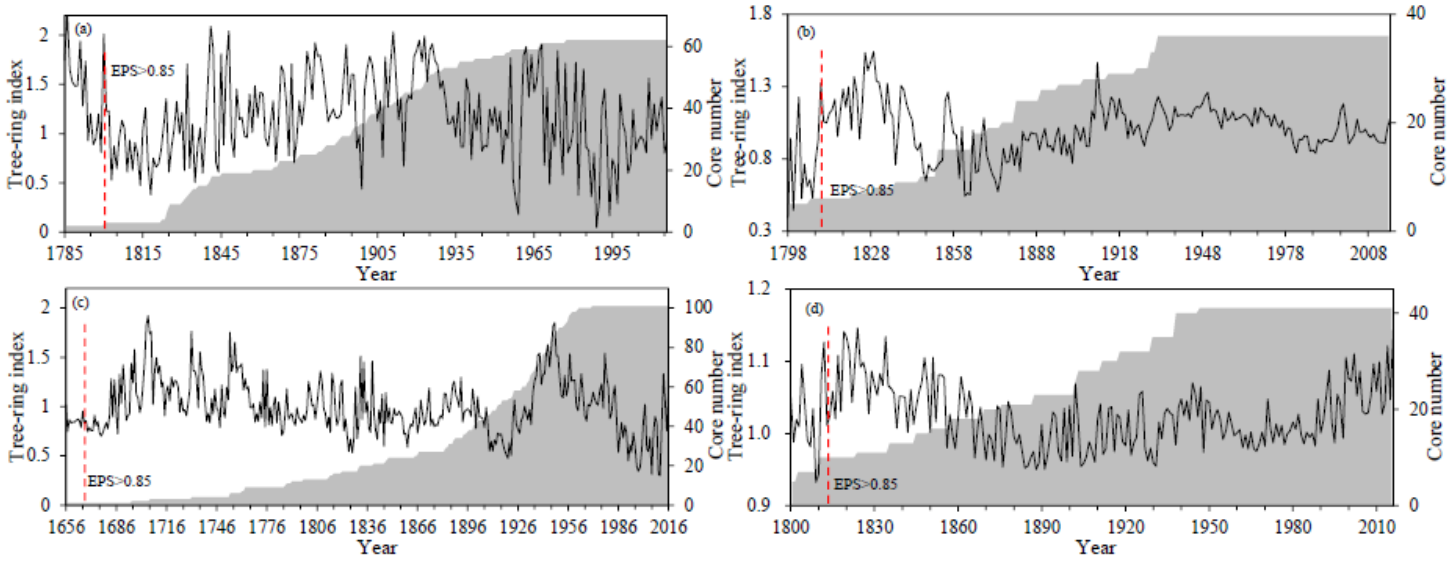

Figure 3

Standardized chronology, sample size, and subsample signal strength of each tree species

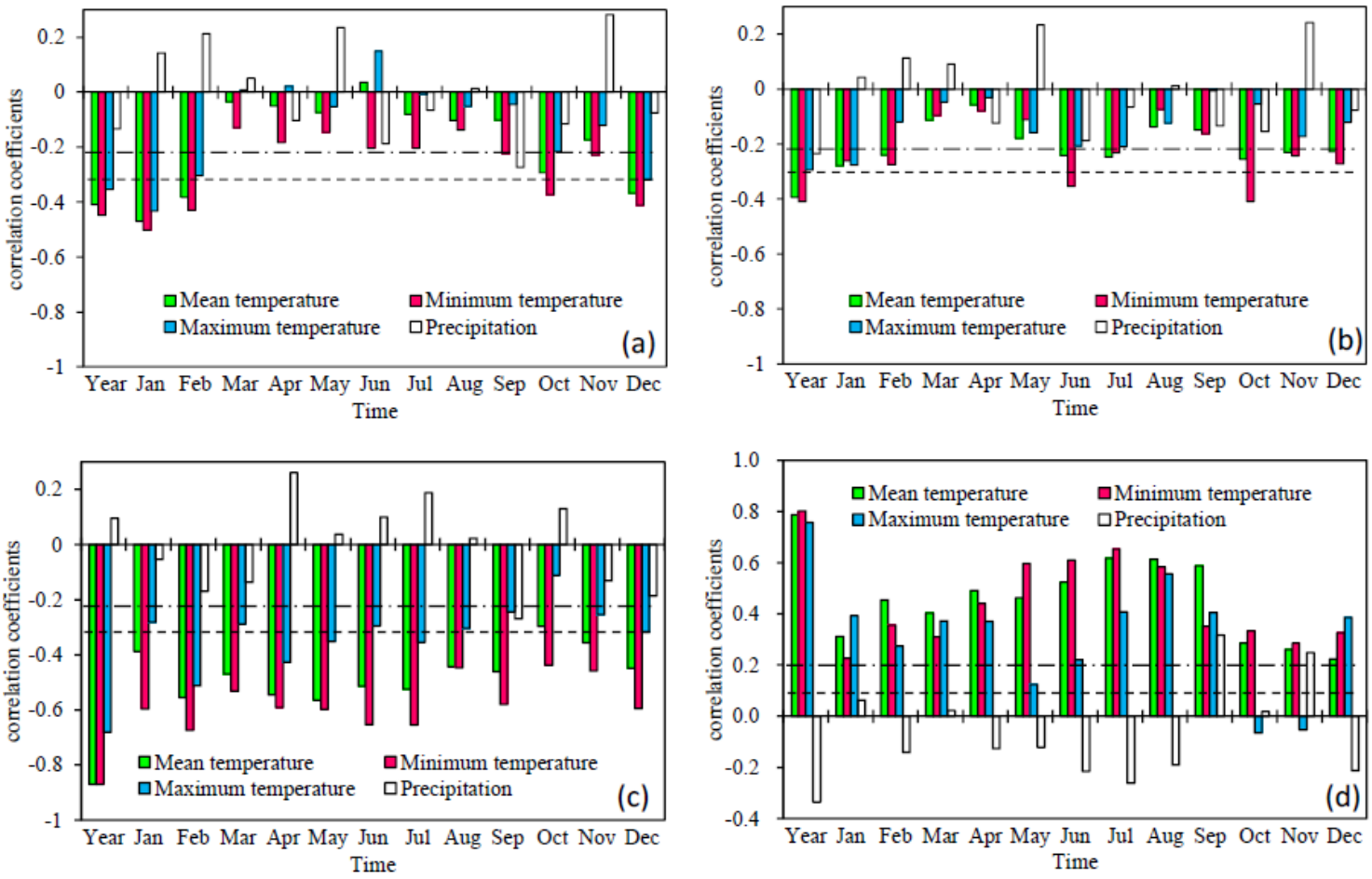

Figure 4

Correlation between the tree-ring index and the annual and monthly climatological factors

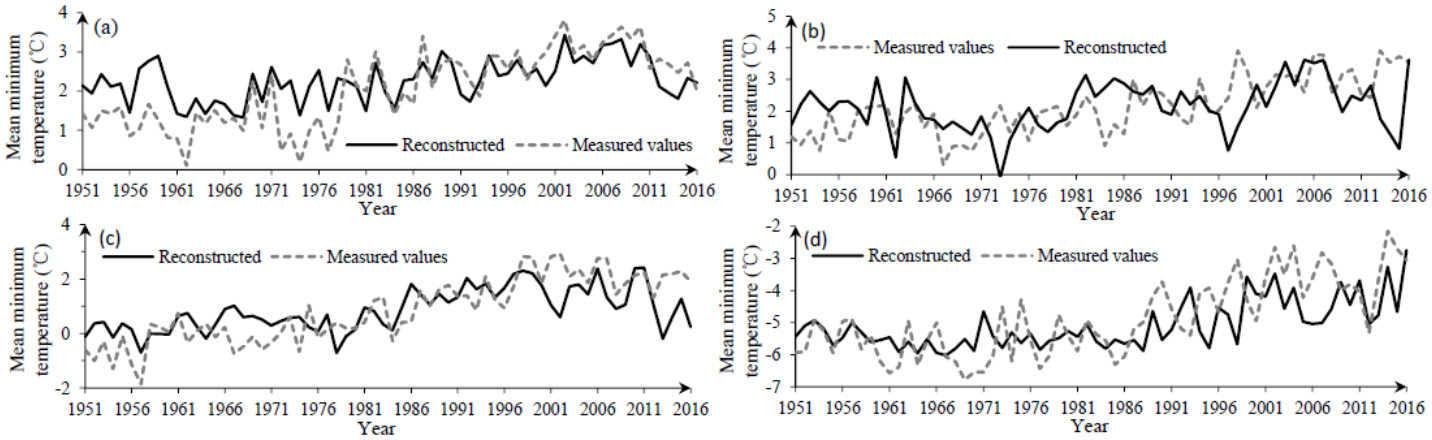

Figure 5

Comparison of the reconstructed and measured values of the annual mean air temperature in each region

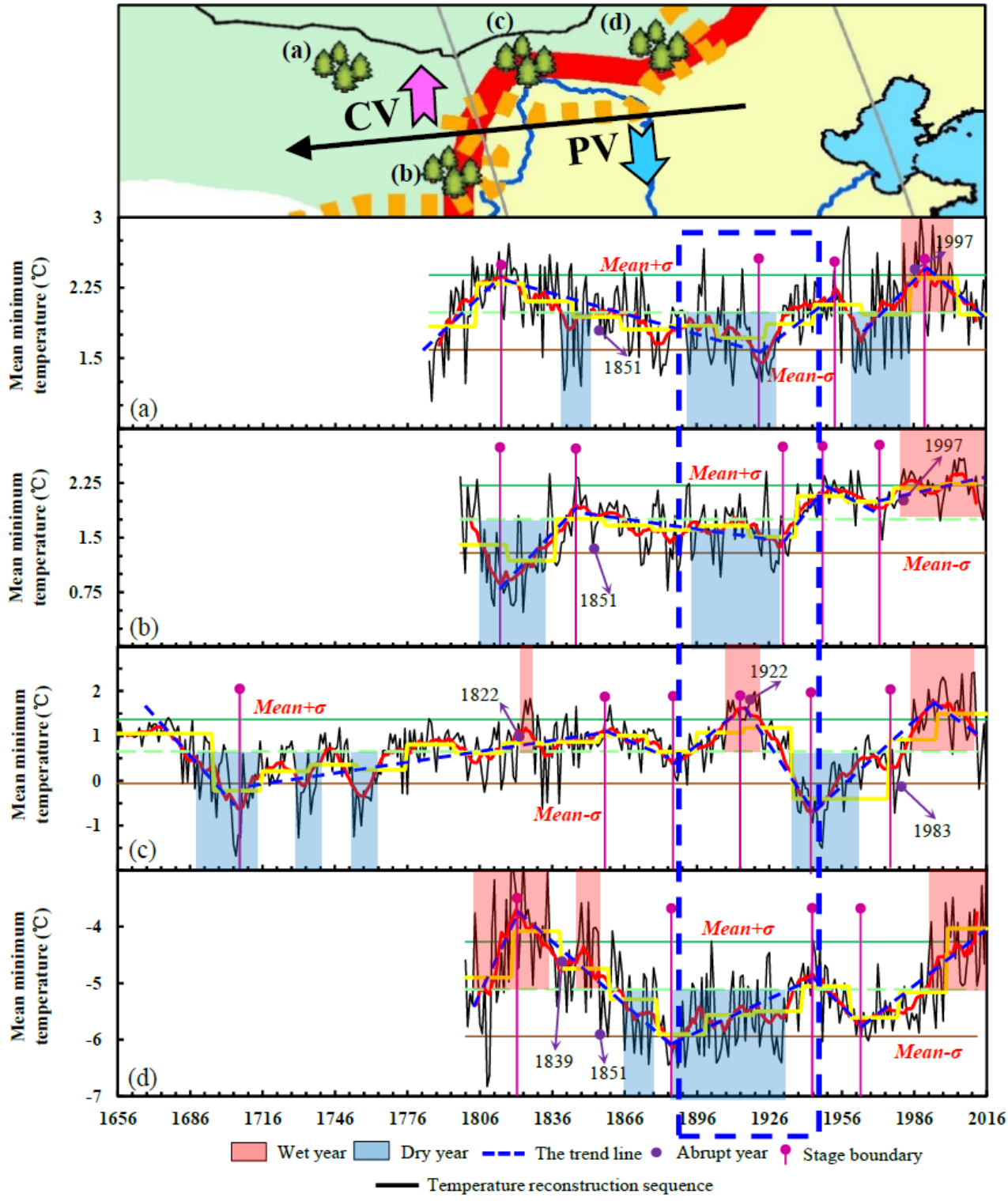

Figure 6

Variability of the reconstructed annual mean minimum temperature series

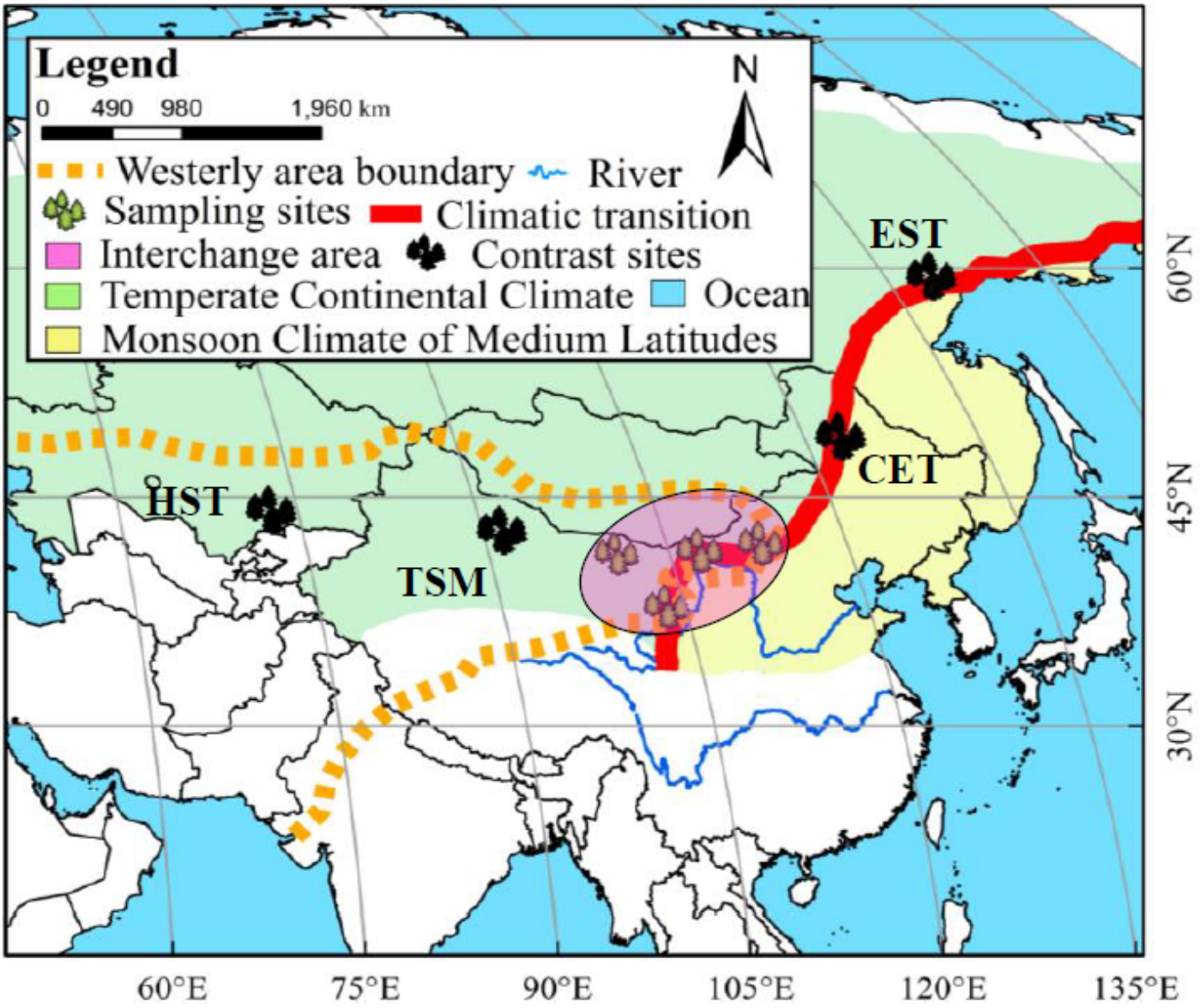

Figure 7

Regions corresponding to the reconstructed series in this study and in other parts of the Asian westerly region and the transition zone corresponding to the existing reconstructed series

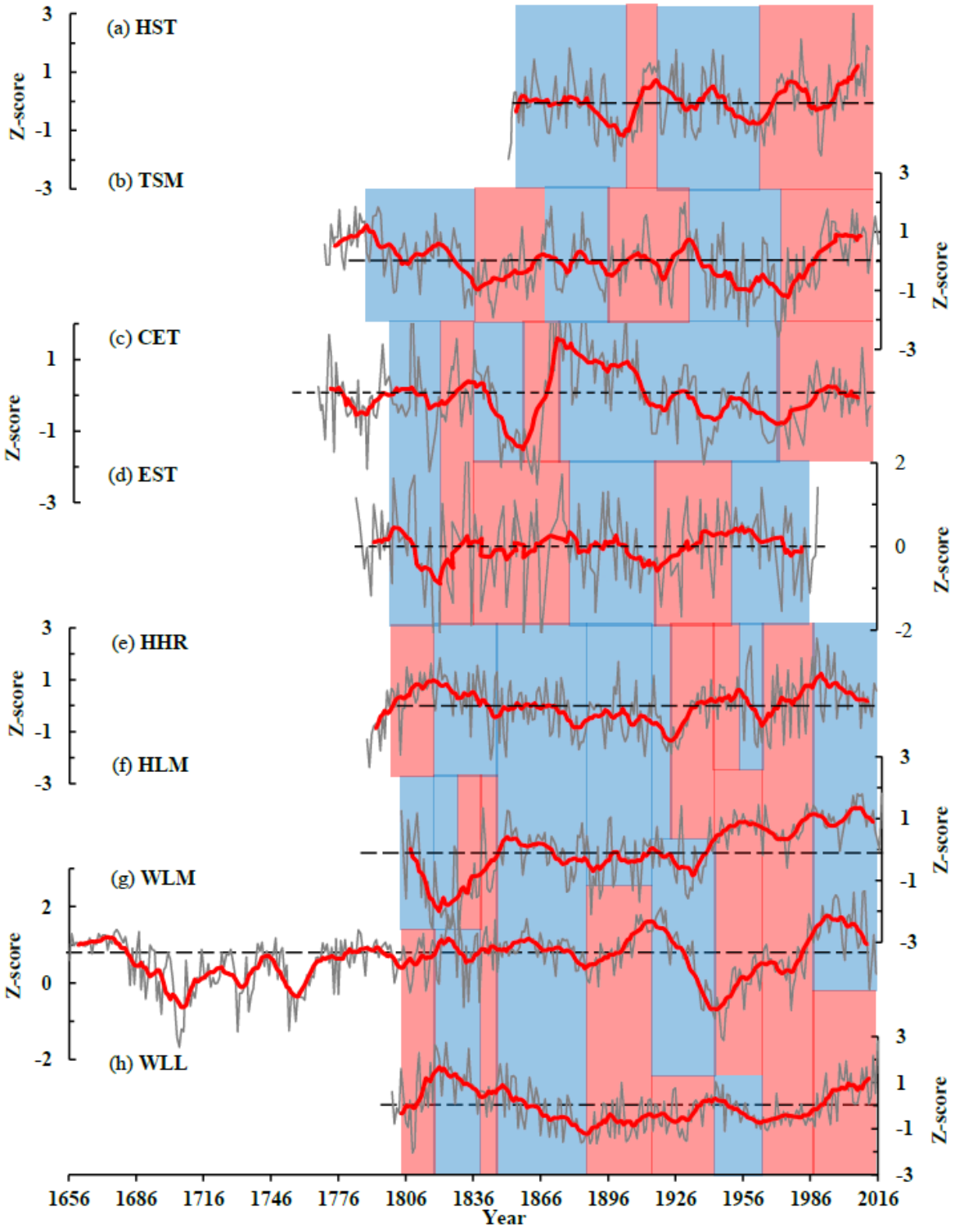

Figure 8

Comparison of reconstructed series in this study with existing reconstructed series in other regions of the overlap region between the Asian westerly region and the transition zone